



Intelligent inspection and quality control of table olives

S. Makni^a • I. Fourati Kallel^{a*} • M. A. Triki^b

^aESSE laboratory, ENET'com, University of Sfax, Tunisia

^bThe Institut of Olive Oil of Sfax, Sfax University, Tunisia

Received 02 03 2024; accepted 07 30 2024

Available 10 31 2024

Abstract: Quality is a key factor of product-marketing in the field of agriculture and food industry. A number of researchers have suggested the use of vision computer systems and machine learning (ML) techniques essentially to inspect imperfection surfaces and defects in fruit products. Following the trend, this paper still relies on the use of vision computer system by assuring an intelligent detection of table olive defect, with a certainty of its quality control. The specifically exploited computer vision system consists of automatically extracting the texture, color, and shape features mainly from the global thresholding segmented image. With reference to the extracted features, the newly introduced system has the capacity to distinguish between the defected and the healthy olive fruits rapidly and effectively at the same time. Subsequently, it is capable of identifying and specifying the diseased table olive. This system is also helpful for estimating the table olive size automatically. The experimental findings are indicative of the high accuracy of the binary classification algorithm, reaching 99, 32%, the average processing time for just one olive is about 0.4 s, which could meet the requirements of the real-time applications, and the error in estimating the size of the table olives does not exceed 10%.

Keywords: Classification, image segmentation, features extraction, size estimation, table olive

*Corresponding author.

E-mail address: imen.fourati@enetcom.usf.tn (I. Fourati Kallel).

Peer Review under the responsibility of Universidad Nacional Autónoma de México.

1. Introduction

Tunisia is ranked as the fourth producer of olives in the world with 172,000 tons per year, after Spain, Italy and Greece. More than one-third of its lands are planted by olive trees with a wide range of varieties (Mehi et al., 2023). Olive cultivation sector is hugely integrated into its economy, even playing important social and environmental roles (Abdallah et al., 2022). It is a determinant factor in the national security of the country by contributing to the Tunisian food security, trade balance and job creation. Olive is one of the most important agricultural products. It is used in various industries, namely oils and pickles ones. The table olive is presumably categorized as a food product, usually consumed either as an appetizer or as a substance in salads, which has a large market primarily in the Mediterranean countries, extended into the whole world. Its homogenous appearance in size and color are critical regarding its marketing to conform with the international standards, and obviously with the absence of defects. Spotting skin damage on table olives is decisive in identifying their out-layered quality as a useful fruit. Traditionally, olives table have been sorted manually based on their external quality. Olive workers, who are responsible for arranging olives into different categories, are positioned on the appropriate sides of the processing line. They inspect the table olive fruits visually and remove those that do not meet the predetermined quality standards. Manual sorting is very dependent on human inspection and interpretation. It is a tedious and time-consuming task, not free from potential errors. It is possible to introduce computer vision methods, which take the place of man power table olive sorting for the sake of increasing the performance of this kind of labor from its different perspectives. This paper presents an intelligent computer vision method, which leads to an extraction of a number of impacting parameters on the olive quality. In addition, it sets out a subsequent categorization of table olives in accordance with their quality. This suggested approach serves to reinforce the efficiency and reliability of quality and size control; meanwhile it ensures speed robustness. The paper's second section represents a modernized work for achieving fruit diseases detection with an inclusion of the sorting and the detection of the olive diseases, in particular. A description of the proposed computer vision system for automatic table olive defect detection and automatic table olive size estimation are detailed in section 3. The following section consists of stating and discussing the main findings. Lastly, the last section includes both concluding remarks and future works.

2. Previous work

Fruit disease detection is a vast area of research. Several studies have been presented to identify fruit diseases and/or defects with the classification of different varieties (Bhole & Kumar, 2020; Shafi et al., 2018). Numerous researches are done to detect and classify diseased olive trees leaves (Kallel et al., 2023). However, few investigations are interested in identifying and classifying the external defects of olives, particularly table olives.

(Riquelme et al., 2008) introduces an automatic method to classify the variety stemming from "Manzanilla sevillana" table olive fruits. The process starts with segmenting the olive image. Next, the color features are extracted. It is finalized with applying three distinctive analyses, which serve to classify the olives into eight classes with an accuracy ranging from 97% to 75%. Hussain Hassan and Nashat (2019) opts for two different algorithms ensuring the distinction between healthy and diseased olive oil. The first algorithm launches a pre-processing step, which improves the quality of the obtained image. It is sequenced with a segmentation step to distinguish the fruits bearing damaged areas from the others. It ends with a classification step, referring to the homogeneity characteristics of the fruits. The second algorithm is applied by using two distinctive convolution masks. A comparison of the convolution findings is led in the light of a fixed threshold to identify the defected olive area. Aguilera Puerto et al. (2019) introduces a ML approach, which serves to classify olive oil into two main classes: tree olive and ground olive. These two classes are used to inspect the oil quality. Nine features are derived by implementing Aguilera's method on the olive fruit image. They are basically five color features from five different color spaces in addition to four texture features from the GLCM matrix. In order to lead an appropriate classification, the author relies on a support vector machine (SVM) and an artificial neural network. The obtained results for both classifiers are openly comparable, with an accuracy of 98.4%.

Alruwaili et al. (2019) suggests a deep learning (DL) method based on Convolutional Neural Network (CNN) architecture called AlexNet in order to identify and then classify 14 different types of olive fruit and leaf diseases with 99.11% accuracy. Figorilli et al. (2022) uses a transfer learning model based on CNN architecture to control the maturity stage and the quality of the olive oil, which in turn, influences the quality of the oil per se. The author subsumed olives under five classes. Actually, the pre-trained network Alexnet was used.

3. Materials and methods

3.1. Samples collection

A database of 148 olive fruits of the Meski cultivator of assorted sizes and shapes are collected. 107 of them are detected and found with different defect types. The remaining 41 are the so-called healthy olives. The olives were previously classified by a set of experts from the Sfax Oil Institute. The camera used to collect all the mentioned samples is known as Canon EOS50D SLR camera with 15.1 megapixel CMOS sensor. It is perpendicularly located above the olive fruit table. In addition, the lights are placed at the same plane and oriented to the focal point by the camera positioning. They are acquired and saved in JPG format, with a color depth of 24 bits, a pixel density of 300 ppi, and a resolution of 256 x 256 pixels, which inversely reduces the background information and increases the salience of the olive fruit table. The distance between the olive and the camera is constant. It is no less than 20 cm whereas the background scene is kept white, which facilitates the activated process. It is worth noting that the acquisition of the images and the collection of the databases of the current work are carried out within the Laboratory of Advanced Electronic Systems and Sustainable Energy of the National School of Electronics and Telecommunications of Sfax.

3.2. Table Olive in Tunisia

Tunisia has a heritage quite rich in cultivars of table olives. The Meski cultivar is the most noticeable one covering 56% of plantations, coming before the 14% of Picholine and the 11% of the Beldi (Debbabi et al., 2022). The cultivar Meski is the variety of olive of table, which is the most cultivated in Tunisia and the most preferred in canning thanks to its detachable pit and its attractive exterior appearance. The fruit is slightly elongated, with an ovoid shape and green color, as shown in figure 2 (c). Economically, the production of table olives is vital for Tunisia. It is one of the most significant, agro-industrial activities. With reference to official statistical data in the International Olive Oil Council 2004, the Tunisian production of olive in 2004 is estimated at 280,000 tons for olive oil and 26,000 tons for the table olive. Table olives are harvested when they reach their maximum size and the appropriate degree of ripeness, normally with green color. The fruit is required to be within the presentation and the commercial standards, complying with the CODEX standard for table olive. The external appearance of a table olive is the most decisive factor in determining its quality, especially for exporting. Concerning Council Oleicol International (COI) COI/OT/NC n° 1 December 2004, there are numerous defects degrading the quality of table olive. Olives of high quality are selected by being distinguished from those that are damaged by a tear in the skin and whose part of the mesocarp becomes visible. Equally, the others which are with marks and defaults

on the external surface, structurally damaged with a changing shape, abnormally wrinkled, or their color affected differently from its normal distinctiveness are kept apart. The present work is basically concerned with the two most damaging pests, causing spots and holes in the table olives through their frequent attacks in the region of Sfax. They are as follows:

- An attack by the black mealy bug of the olive tree can definitively damage the plant. It feeds on the sap of the plant, causing its weakness and probably an appearance of a black fungus called fumagine on it. The attack of the mealybug on the olives is featured by the appearance of black spots encircled with purple.
- The olive fly (*Bactrocera oleae*) (Daane & Johnson, 2010), which is small and 5 mm long, attacks an olive when it is formed around the month of July by stinging it to deposit its eggs. This attack causes the appearance of black holes, as traces of stings. They are shown in figure 2 (a). The existence of worms inside an olive stems from the fly laying eggs in the attacked olive.

Generally, table olive diseases are the main causes of different acute problems. They deeply affect the economy of the table olive producing countries as well as the worldwide agricultural industry. For these reasons, the earlier detection of the olive diseases, the better their treatments is. Most farmers use traditional methods to identify olive diseases, notably visual inspection or even laboratory examination. Unlike nowadays, artificial intelligence techniques have been introduced as effective methods for the automatic detection and classification of table olive diseases. These newly invented techniques are considered as an efficient alert to draw the farmers' attention before the spreading of the disease over large areas.

3.3. Computer vision system

Presumably, computer vision is recently an ideal way to meet the inspectional objectives, to check quality consistently, and to reduce the tedious tasks done by laborers. This section is mainly a description of the distinctive technique of the proposed intelligent computer vision system. It is essentially designed to sort and calibrate table olives according to their quality, shape, and color. This technique guarantees a high detection as well as classification efficiency. It is used to keep away the undesirable olives such as those occurring with different types of defects, the damaged, the overripe or those which are harvested from the ground. These anomalous olives are obviously and necessarily prevented from the marketing phase, which keeps the olives' quality of a great commercial value.

The prototypical design of the computer vision system shown in figure 1 is made up of four basic components: lighting, a capturing image camera, image processing software, and computer hardware. At the time of reception, two successive preparatory steps are followed: firstly, waste elimination; and

secondly, small size fruit exclusion by calibration. Subsequently, the quality check procedures are pursued in addition to the classification of olive. The received table olives are initially poured onto the conveyor belt. The olives pass through vibrating sieves to get rid of sand, and small stones as intruding substances, and a special fan to remove the leaves. The calibration is a step of separating olives in the light of their sizes. This operation is done by a conveyor belt above which there is diverting cables row, which excludes the small olives. It is noticed that the table olives are very sensitive to the point that the final product, with respect to quality, may be negatively influenced by defects such as disease, deformation, or inadequate method of harvesting. This is why olives go through a sorting step for the separation of green olives by quality. The images are taken under artificial lighting, which is accessed by fluorescent lamps. Once the table olives are acquired, they are transferred to a PC. At this level, the olives are processed and divided into two categories with reference to their defects and standard tolerance.

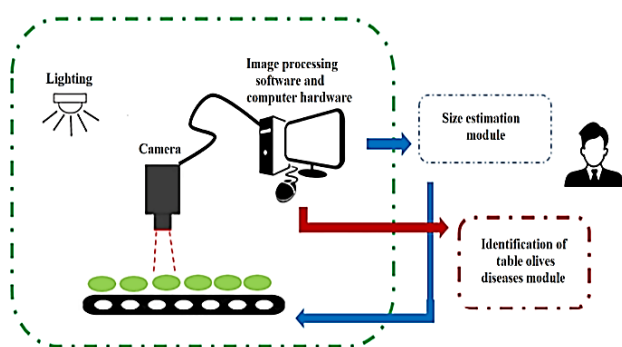


Figure 1. Computer vision system.

3.4. Image processing software

This application is composed of three main steps: firstly, the table olive image goes through thresholding segmentation phase. Secondly, the shape, color, and texture features of the olive image are calculated. Ultimately, the extracted features are gone through a binary SVM classifier. The image processing software displays two modules independent from the main chain: the first is for the table olive fruit size estimation while the second is for the olive diseases type identification. These modules are separately applied to avoid any slowing down of the main application since time constraint is of paramount importance. The module of the olive fruit size estimation is used mainly for adjusting the mechanical method. The other module of the table olive disease identification is applied to the olives, which have already been discarded by the main applications. Accordingly, an early diagnosis and checking of the table olives pests and diseases are essential to avoid yield losses. Evidently, the olives that are found with anomalies are gone through a second classification. It is detected to find any kind of diseases

in order to collect statistical data for examination and/or inform farmers of the olives' quality. These procedures are proven to be valid for alerting farmers of the olives' conditions earlier, before spreading of the disease over large areas.

3.4.1. Global thresholding segmentation

Global thresholding segmentation method is applied in this section. It is used to search for the appropriate threshold in order to separate the olive fruit from the background. Indeed, the Otsu method is used.

The HSV color space is more effective for color texture analysis (Paschos, 2001). Hence, the table olive image is converted from the RGB color space to the HSV color for the purpose of facilitating the segmentation-processing (Prema et al., 2012). The saturation channel is considered as the input image in the thresholding segmentation process. This channel is elementary selected to make a crystal clear distinction of the olive characteristics, particularly the defects, the anomalies, and the suspicious regions.

The Otsu method (Kallel et al., 2024) is practically useful for the selection of the optimal threshold T_{opt} , which maximizes the inter-class variance σ_B^2 , defined as follow:

$$\sigma_B^2 = w_0(\mu_0 - \mu_{total})^2 + w_1(\mu_1 - \mu_{total})^2 \quad (1)$$

Where w_0 and w_1 are the class probabilities, μ_0 and μ_1 are the class mean and μ_{total} is the total mean level of the original image.

The olive fruit is extracted from its background during the segmentation process, where the green table olive is successfully extracted with a white appearance. The gray level masks are also estimated as shown in figure 2. This resultant mask is an image representing the fruit with gray intensity and background as black pixels.

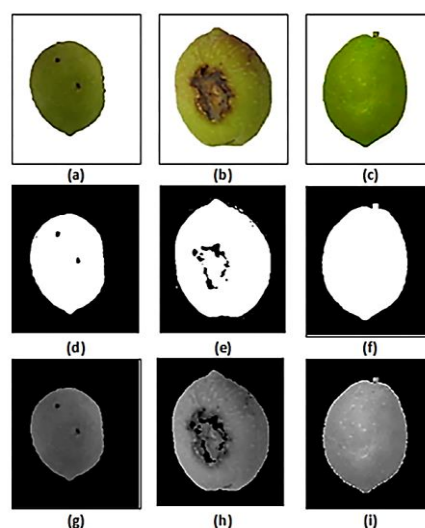


Figure 2. Segmentation results: (a), (b), and (c) are the original olive images. (d), (e) and (f) are the segmented images, and (g), (h) and (e) are the gray level masks.

3.4.2. Feature extraction

The feature extraction step is designed to provide compact, non-redundant and meaningful information of the olive image. In order to describe the olive fruit texture, color and shape features are extracted from the table olive image. The shape of the fruit is critical in relation to the quality parameter. In turn, it affects the aesthetic appearance and the table olives marketability.

In this work, two shape features of the table olive are extracted using the segmented image; the fruit shape index (FSI) and Polsby-Popper Score (PPS). The FSI (Wu et al., 2018) is the ratio of width to length of the fruit. The bounding box method (Wang et al., 2018) is used as shown in figure 3(c). The PPS (Polsby et al., 1991) measures the compactness of the shape; it is calculated using equation (2):

$$PPS = \frac{4 * \pi * area}{(Perimeter)^2} \quad (2)$$

As shown in figure 3(a), the perimeter and the area of the table olive are derived from the segmented image.

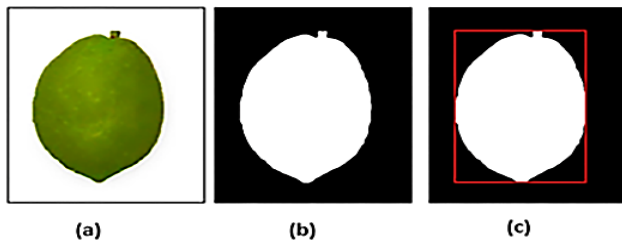


Figure 3. (a) Original image, (b) Segmented image, (c) Minimum bounding box.

Color is a commonly used feature for plant, vegetables and fruit recognition artificial vision systems due to its simplicity of extraction and low computational cost. Because of their green appearances, the G channel is used as the main channel to extract the color feature. The green mean value (GMV) is defined as:

$$GMV = \frac{1}{N} \sum_{i=1}^n G(i) \quad (3)$$

where G(i) is the value of the green channel at the ith index of the olive image and n represents the total number of pixels in the image. With a high GMV's value, an olive is not considered defective. However, if the value is low the fruit is counted as abnormal.

Statistical features are used to describe the table olives fruit texture aspect. The first order uniformity and entropy (Kshirsagar et al., 2020) are used for the purpose of distinguishing the altered olive from the normal one. In this respect, the healthy olive has a homogeneous texture. In the same context, entropy is an effective measure of image randomness.

$$Uniformity = \sum_{i=0}^{L-1} [(P(z_i))]^2 \quad (4)$$

$$Entropy = - \sum_{i=0}^{L-1} P(z_i) \log_2 P(z_i) \quad (5)$$

Where z_i is a random variable representing the intensity levels of the image, $P(z_i) = \frac{n(z_i)}{N}$ is the normalized histogram of intensity levels, $i = 0, \dots, L$, and L is the number of distinct possible intensity levels. N is the total number of pixels in an image.

The second order is more informative about the table olive texture. More information about it is provided in order not only to know how to identify the different anomalies but also to specify the table olive diseases. Since the statistical characteristics of second order are also used. Four gray level co-occurrence matrix (GLCM) are calculated to describe the image texture in the 0°, 90°, 45° and 135° directions (Thomas et al., 2019). The distance d is set to 1. The three second-order texture analysis features of homogeneity, correlation, and entropy (Kshirsagar et al., 2020) are selectively implemented. The mathematical description of the examined features is embodied in equation (6), (7), and (8) below:

$$Homogeneity = \sum_i \sum_j \frac{C(i,j)}{1+(i-j)^2} \quad (6)$$

$$Entropy = - \sum_i \sum_j P_{i,j} \ln(C(i,j)) \quad (7)$$

$$Correlation = \sum_i \sum_j \frac{C(i,j)(i-\mu_i)(j-\mu_j)}{\sigma_i \sigma_j} \quad (8)$$

Where μ_i and μ_j represent the mean of the rows and the columns of the GLCM matrix respectively; σ_i and σ_j the standard deviations of the rows and the columns of the GLCM matrix respectively. C(i,j) is the coefficient of the co-occurrence matrix. In this work the GLCM matrix is 2 x 2 with four cells. As it seems in the binary-segmented image, there are merely two values, which are represented by 0 and 1.

The application of the GLCM to the binary image resulting from the segmentation simplifies the necessary calculation. The 2x2 GLCM is aimed to specify the defected/healthy classification, which is actually implemented to use the suggested computer vision system in real time, avoiding a long calculation. However, concerning the disease identification and classification block, which is out of the circle of the real time application, with no real time control, the GLCM are applied to the gray extracted masks in order to get more significant texture features.

3.4.3. Classification

The obtained vector feature is given as an input in the classification process. The SVM is one of most successful classifiers (Zhang et al., 2006). The SVM maps the training data in an N-dimensional space, with N signifying the number of

features. Then, it separates the two classes of data with a hyper-plane, minimizing the distance termed the margin. It is possible to estimate the function of the SVM classifier hyper-planes by:

$$F(x) = \text{sgn}(w^T x + b) \quad (9)$$

where $w \in R^p$ and $b \in R$ w and b are given by solving the following problem:

$$\text{Minimize } \frac{1}{2} \|w\|^2 \quad \text{With } y_i(w^T x_i + b) \geq 1 \quad (10)$$

$$i = 1, n$$

Such that $\{(x_i, y_i); i = 1, n\}$ a set of shape vectors labeled with $x_i \in R^p$ and $y_i \in \{1, -1\}$

3.4.4. Size olive estimation module

The purpose of this section is to automatically predict the table olive fruit size through the image processing techniques. The basic requirement is having table olives with uniform size. To adjust the mechanical olive calibration device a verification process based on image processing is provided.

The bounding box method (Wang et al., 2018) is used in this work. A_e the estimated area of table olive is the product of L and W , respectively the length and width of the drawn rectangle. The olive table automatic estimated area is compared to a fixed size threshold (ST). The ST is defined and controlled by experts according to the desired standard and category of the table olive sorting. Numerous categories have been detailed in the Codex Alimentarius table olive standards.

4. Results and discussion

In this section, the classification accuracy, the computation time and the size estimation results of the proposed computer vision system are presented in detail with discussion.

4.1. Classification results

The images of the olive are randomly split into training and test set with a ratio of 70% to 30%. Four metrics are used to verify the classification process performance, which are accuracy (Kallel Fourati et al., 2024), precision, recall, and F1 score (Grandini et al., 2020). Eight features are extracted from the olive fruit images to train and test the SVM classifier. These features are normalized within the range of [0 1], using the max-min method (Ali et al., 2014) and then used as input to the SVM classifier. A first classification is used to differentiate between healthy olives and anomalous ones in order to guarantee a good quality of the product.

The classification model is trained and consequently tested using a 5-fold cross-validation technique to avoid overfitting problems. The average classification performances results are represented in table 1.

Table 1. Classification performances.

	Accuracy	Recall	Precision	F1score
Classification 1	99.32 %	97.61%	100 %	0.987
Classification 2	96.26%	96.77%	96.77%	0.967

The classification performance shows a reasonable consistency. As it is demonstrated in table 1, the system can sort 99.32% olive accurately, which proves the proposed computer vision application effectiveness. The recall of the classification is 97.61%. In turn, it wrongly classified a healthy image as defected. The classification precision is 100%, which proves that the system has left no error of false positive type. The proposed quality control system perfectly guarantees no escape of defective olives escape. Olive table fruits with marks or superficial stains, which affect the appearance of the consumption quality, are not going to be thrown away. Rather, they are crushed and transformed into oil. The found F1 score value of 0.987 confirms the classification process effectiveness.

Table olive diseases can cause huge damage to this type of fruit whose external appearance and quality are critically decisive for its marketing. The earlier table olive diseases detection and preventive measures, the lower the risk of the infectious spread is. Developed techniques for an automatic olive disease detection and classification by olive image processing are noticeably required. The second independent module used out of the industrial chain circle serves the table olive diseases identification for classification purposes. During classification, a distinction is made between the images of olives attacked by the mealy bug and those by the olive fly. The results presented in table 1 indicate that the olive disease classification module gives promising results with an accuracy of 96.26%, a recall of 96.77% and precision of 96.77%.

4.2. Computation time

Computation time is an important factor in evaluating the table olive classification. In order to measure the total process time, the processing time for each step of the algorithm is evaluated. Five images are randomly selected from the used database. For each 256×256 image, the average processing time for the pre-processing time step, global thresholding segmentation, feature extraction and SVM normal/abnormal classification is shown in table 2. The SVM training time is not considered since the used parameters remain unchanged after training.

The computation time of the table olive size estimation and the identification of the olive disease are not taken into consideration; these two steps are independent of the computer vision application in real time. In fact, they are two operations, which may be implemented once they are

needed. As shown in table 2, the total processing time is about 0.4s. It could meet the real time applications requirements. Then, the results are more promising than those reported in the literature, notably the approaches of Liming and Yanchao (2010) and Bato et al. (2000), that classified strawberries with an average time of three and one seconds for one fruit respectively.

Table 2. Computation time (s) for each of the image processing steps using 5 randomly selected images.

Operations		Time (s)
Pre-processing	Image resize	0.003314
	RVB-HSV color space conversion	0.009637
Image segmentation	Global thresholding	0.004918
Features extraction	Texture features	0.102564
Classification	Binary SVM	0.265400
Total processing time		0,385833

4.3. Size estimation

To evaluate the size estimation module performance, the objective measurements of the width and the length in millimeters are made for each olive table image. The vernier caliper is used to measure the external size of the olive table fruit. To get the width and the length of the table olive, the fruit is placed between the jaws of the caliper. The sliding jaw is then moved until the olive is firmly grasped between the jaws as shown in figure 4.

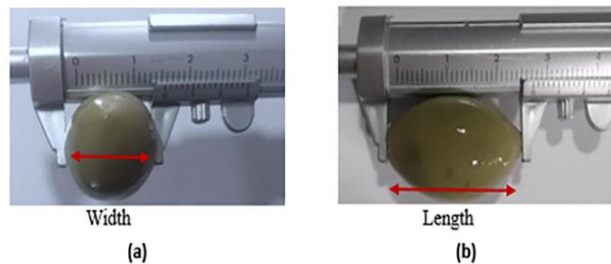


Figure 4. Table olive size measuring with a vernier caliper.

Then, the width and the length of 20 table olive samples are estimated using the automatic visual measurement technique, which are subsequently compared to the manually assessed ones. Table 3 illustrates a comparison between the automatic visual length and width measurement of the table olives size and the real length and width measurement of 5 samples as elaborated examples. Size in pixel units is transformed to millimeters through the calibration factors,

which depends on the distance between the camera and the table olive. The calibration factor of 0.12mm /pixel for any olive fruit, taken from a constant distance of 20 cm, is found by using spatial calibration, which involves calibrating a single image against known values. Next, the calibration is applied to the other non-calibrated images.

Table 3. Comparison between automatic visual measurement of the size of table olives and real measurement.

Samples	Automatic visual measurement		Actual measurement	
	Length	Width	Length	Width
1	23	15,7	22,9	15,7
2	25,4	16	25,5	16,1
3	23,3	15,6	23,4	15,7
4	23,5	15,9	23,3	15,8
5	23,2	15,6	23,4	15,7

The displayed results in table 3 prove that the estimated size with the proposed method is so close to the real size measurement of the olive table. The error does not exceed 10%, compared to the real measurement. The maximum difference is 3 mm between the two measurements. These errors refer to measuring the olive table length and the width with the vernier caliper. There may be some other intervening variables, which have an impact on the measurement errors notably, the location and configuration of the camera itself. The obtained measuring results are normally acceptable. However, they can be improved by using a more sophisticated digital caliper, a better camera configuration, and the perfectible calibration. The coefficient of determination R^2 (Rodríguez Sánchez et al., 2022) and the root mean squared error RMSE (Hodson, 2022) are used to evaluate the relationship between the real and the automatic estimated measure. The R^2 and the RMSE are calculated using the just below formula:

$$R^2 = 1 - \frac{\sum_{i=1}^n (y_i - \hat{y}_i)^2}{\sum_{i=1}^n (y_i - \bar{y})^2} \tag{11}$$

$$RMSE = \sqrt{\frac{1}{n} \sum_{i=1}^n (\hat{y}_i - y_i)^2} \tag{12}$$

Where n is the number of studied samples, y_i the real measurement, the corresponding automatic visual measurement \hat{y}_i and \bar{y} the mean of the measurements.

The findings are configured by $R^2 = 0,861$ and $RMSE = 0,162$ mm for the length measurement while $R^2 = 0,985$ and $RMSE = 0,1549$ mm for width one. They imply a strong correlation with no significant error between the means of the real and the

measured values. The findings are promising again with a more and more approximation to the real olives table size.

In comparison with the findings of the classification performance for methods cited in the state of the art section, the current results of this study outperform those of Shafi et al. (2018), Riquelme et al., (2008) and Aguilera Puerto et al. (2019); and are comparable to those of the Alruwaili et al. (2019) deep learning method. Indeed, the DL method already cited in the state of the art section uses the classic CNN model, or others whose mechanisms are derived from the CNN's itself, namely the AlexNet model (Alruwaili et al., 2019) and the SqueezeNet model (Bhole & Kumar, 2020). These DL models require many parameters, with complicated mathematical formulas. On the one hand, the computation time system is elevated. On the other hand, the training network requires a huge data set. In this respect, the DL models require very powerful machines whose hardware is sturdy and resources are valuable. This fact proves that the presently used ML approach, which has a simple structure, is more efficient. It is quickly set up with less time to train since the data sets are smaller. Moreover, extract features from the resulting binary image segmentation facilitate the calculating operations, particularly for the second order characteristics where the size of the GLCM matrix depends on the number of image intensity levels. Furthermore, the linear binary SVM classifier is considered to be one of the fastest classification algorithms. Two separated modules are used to identify the size estimation and the table olive disease. These two modules, which are implemented separately, do not slow down the industrial process. The obtained results indicate that the proposed computer vision system has a great potential for use in a real industrial environment. The presented computer vision system performance outperforms the computer vision ones, which are cited in the literature. This is not only in terms of classification accuracy, but also in terms of computation time, simplicity and precision in fruit size estimation.

5. Conclusions

This study proposes an efficient computer vision system for table olive control quality based on the artificial intelligence technique. It reveals a new design and an implementation of a prototype classification and sorting system of table olive. The system uses the RGB images of table olives from where color, shape, and texture features are automatically extracted. Regarding the extracted characteristics, the proposed system offers a useful classification of table olives by subsuming them under two categories: the healthy and the defective. Two separate modules for size estimation and disease identification of table olives are also implemented. It is possible to extend the presently developed method into future works. Seemingly, it proves to be very useful with other

fruit varieties for similar sorting and grading applications in the food industry, which are the same as the olives oil, particularly other fruits with similar characteristics of size and shape. The performance of the proposed approach can also be evaluated by putting other table olive anomalies under investigation. To improve the proposed real time computer vision application, the possibility of parallel execution is practicably required. Hence, thanks to the current microprocessors with two or four computing cores and the Parallel Computing Toolbox (PCT), parallel applications can be easily developed in MATLAB. This calculation type, which embeds several calculations, can be performed simultaneously with the advantage of reducing the computation time considerably.

Conflict of interest

The authors have no conflict of interest to declare.

Acknowledgements

The authors thank the staff of the Sfax Olive Oil Institute for the generous help by offering olive samples, technical support, and results validation.

Funding

The authors received no specific funding for this work.

References

- Abdallah, S. B., Parra-López, C., Elfkih, S., Suárez-Rey, E. M., & Romero-Gómez, M. (2022). Sustainability assessment of traditional, intensive and highly-intensive olive growing systems in Tunisia by integrating Life Cycle and Multicriteria Decision analyses. *Sustainable Production and Consumption*, 33, 73-87.
<https://doi.org/10.1016/j.spc.2022.06.022>
- Aguilera Puerto, D., Cáceres Moreno, Ó., Martínez Gila, D. M., Gómez Ortega, J., & Gámez García, J. (2019). Online system for the identification and classification of olive fruits for the olive oil production process. *Journal of Food Measurement and Characterization*, 13, 716-727.
<https://doi.org/10.1007/s11694-018-9984-0>
- Ali, P. J. M., Faraj, R. H., Koya, E., Ali, P. J. M., & Faraj, R. H. (2014). Data Normalization and Standardization: a Technical Report. *Mach Learn Tech Rep*, 1(1), 1-6.
<https://doi.org/10.13140/RG.2.2.28948.04489>

- Alruwaili, M., Alanazi, S., Abd El-Ghany, S., & Shehab, A. (2019). An efficient deep learning model for olive diseases detection. *International Journal of Advanced Computer Science and Applications*, 10(8).
<http://dx.doi.org/10.14569/IJACSA.2019.0100863>
- Bhole, V., & Kumar, A. (2020). Mango quality grading using deep learning technique: Perspectives from agriculture and food industry. In *Proceedings of the 21st annual conference on information technology education* (pp. 180-186).
<https://doi.org/10.1145/3368308.3415370>
- Daane, K. M., & Johnson, M. W. (2010). Olive fruit fly: managing an ancient pest in modern times. *Annual review of entomology*, 55(1), 151-169.
<https://doi.org/10.1146/annurev.ento.54.110807.090553>
- Debbabi, O. S., Amar, F. B., Rahmani, S. M., Taranto, F., Montemurro, C., & Miazzi, M. M. (2022). The status of genetic resources and olive breeding in Tunisia. *Plants*, 11(13), 1759.
<https://doi.org/10.3390/plants11131759>
- Figorilli, S., Violino, S., Moscovini, L., Ortenzi, L., Salvucci, G., Vasta, S., ... & Pallottino, F. (2022). Olive fruit selection through ai algorithms and RGB imaging. *Foods*, 11(21), 3391.
<https://doi.org/10.3390/foods11213391>
- Grandini, M., Bagli, E., & Visani, G. (2020). Metrics for multi-class classification: an overview. *arXiv preprint arXiv:2008.05756*.
<https://doi.org/10.48550/arXiv.2008.05756>
- Hodson, T. O. (2022). Root-mean-square error (RMSE) or mean absolute error (MAE): when to use them or not. *Geoscientific Model Development*, 15(14), 5481-5487.
<https://doi.org/10.5194/gmd-15-5481-2022>
- Hussain Hassan, N. M., & Nashat, A. A. (2019). New effective techniques for automatic detection and classification of external olive fruits defects based on image processing techniques. *Multidimensional Systems and Signal Processing*, 30, 571-589.
<https://doi.org/10.1007/s11045-018-0573-5>
- Kallel, I. F., & Kammoun, S. (2024). Hybrid human-artificial intelligence system for early detection and classification of AMD from fundus image. *Signal, Image and Video Processing*, 18(5), 4779-4796.
<https://doi.org/10.1007/s11760-024-03115-2>
- Kallel, I. F., Kallel, M., Ghorbel, M., & Triki, M. A. (2023). Smart Farming: Automatic Detection and Classification of Olive Leaf Diseases. In *Handbook of Research on AI Methods and Applications in Computer Engineering* (pp. 316-338). IGI Global.
<https://doi.org/10.4018/978-1-6684-6937-8.ch015>
- Kallel Fourati, I., & Kammoun, S. (2024). A matlab based graphical user interface for the monitoring and early detection of keratoconus. *Journal of Applied Research and Technology*, 22(1), 22-31.
<https://doi.org/10.22201/icat.24486736e.2024.22.1.2103>
- Kshirsagar, P. R., Yadav, A. D., Joshi, K. A., Chippalkatti, P., & Nerkar, R. Y. (2020). Classification and detection of brain tumor by using GLCM texture feature and ANFIS. *J. Res. Image Signal Processing*, 5, 15-31.
<http://doi.org/10.5281/zenodo.3732939>
- Liming, X., & Yanchao, Z. (2010). Automated strawberry grading system based on image processing. *Computers and electronics in agriculture*, 71, S32-S39.
<https://doi.org/10.1016/j.compag.2009.09.013>
- Mechi, D., Pérez-Navado, F., Montero-Fernández, I., Baccouri, B., Abaza, L., & Martín-Vertedor, D. (2023). Evaluation of Tunisian olive leaf extracts to reduce the bioavailability of acrylamide in Californian-style black olives. *Antioxidants*, 12(1), 117.
<https://doi.org/10.3390/antiox12010117>
- Bato, P. M., Nagata, M., Cao, Q., Hiyoshi, K., & Kitahara, T. (2000). Study on Sorting System for Strawberry Using Machine Vision (Part 2) Development of Sorting System with Direction and Judgement Functions for Strawberry (Akihime variety). *Journal of the Japanese Society of Agricultural Machinery*, 62(2), 101-110.
<https://doi.org/10.11357/jsam1937.62.100>
- Paschos, G. (2001). Perceptually uniform color spaces for color texture analysis: an empirical evaluation. *IEEE transactions on Image Processing*, 10(6), 932-937.
<https://doi.org/10.1109/83.923289>
- Polsby, D. D., & Popper, R. D. (1991). The third criterion: Compactness as a procedural safeguard against partisan gerrymandering. *Yale L. & Pol'y Rev.*, 9, 301.
<http://dx.doi.org/10.2139/ssrn.2936284>
- Prema, C., & Manimegalai, D. (2012). Survey on skin tone detection using color spaces. *International Journal of Applied Information Systems*, 2(2), 18-26.

Riquelme, M. T., Barreiro, P., Ruiz-Altisent, M., & Valero, C. (2008). Olive classification according to external damage using image analysis. *Journal of Food Engineering*, 87(3), 371-379.
<https://doi.org/10.1016/j.jfoodeng.2007.12.018>

Rodríguez Sánchez, A., Salmerón Gómez, R., & García, C. (2022). The coefficient of determination in the ridge regression. *Communications in statistics-simulation and computation*, 51(1), 201-219.
<https://doi.org/10.1080/03610918.2019.1649421>

Shafi, A. S. M., Rahman, M. B., & Rahman, M. M. (2018). Fruit disease recognition and automatic classification using MSVM with multiple features. *International Journal of Computer Applications*, 181(10), 104934.
<https://doi.org/10.5120/ijca2018916773>

Thomas, R., Qin, L., Alessandrino, F., Sahu, S. P., Guerra, P. J., Krajewski, K. M., & Shinagare, A. (2019). A review of the principles of texture analysis and its role in imaging of genitourinary neoplasms. *Abdominal Radiology*, 44, 2501-2510.
<https://doi.org/10.1007/s00261-018-1832-5>

Wang, Z., Koirala, A., Walsh, K., Anderson, N., & Verma, B. (2018). In field fruit sizing using a smart phone application. *Sensors*, 18(10), 3331.
<https://doi.org/10.3390/s18103331>

Wu, S., Zhang, B., Keyhaninejad, N., Rodríguez, G. R., Kim, H. J., Chakrabarti, M., ... & Van der Knaap, E. (2018). A common genetic mechanism underlies morphological diversity in fruits and other plant organs. *Nature communications*, 9(1), 1-12.
<https://doi.org/10.1038/s41467-018-07216-8>

Zhang, X., Krewet, C., & Kuhlenkötter, B. (2006). Automatic classification of defects on the product surface in grinding and polishing. *International Journal of Machine Tools and Manufacture*, 46(1), 59-69.
<https://doi.org/10.1016/j.ijmachtools.2005.03.013>